

¹ Prediction of Extreme Geomagnetically Induced ² Currents in the UK high-voltage network

Ciarán D. Beggan,¹ David Beamish,¹ Andrew Richards,² Gemma S. Kelly¹

and Alan W.P. Thomson¹

Corresponding author: C. D. Beggan, British Geological Survey, Murchison House, West Mains Road, Edinburgh, EH9 3LA, UK. (ciar@bgs.ac.uk)

¹British Geological Survey, UK.

²Market Operation, National Grid Ltd,
UK.

3 **Abstract.** Geomagnetically Induced Currents (GIC) can be damaging
4 to high-voltage power transmission systems. GIC are driven by rapid changes
5 in the strength of the magnetic field external to the Earth's surface. Elec-
6 tric fields are produced in the ground by the interaction between this chang-
7 ing magnetic field, the sea and the conductivity structure of the Earth. Us-
8 ing a technique known as the 'thin-sheet approximation' we can determine
9 the electric field at the Earth's surface, which in turn allows the calculation
10 of GIC in the earthing connections of high-voltage transformers within a power
11 grid. This paper describes two new developments in the modelling of GIC
12 in the UK, though the results are applicable to GIC-related research in other
13 regions. Firstly, we have created an updated model of the UK surface con-
14 ductivity by combining a spatial database of the UK geological properties
15 (i.e. rock type) with an estimate of the conductivity for specific formations.
16 Secondly, we have developed and implemented a sophisticated and up-to-date
17 model for the 400 kV and 275 kV electrical networks across the whole of Great
18 Britain and, in addition, the 132 kV network in Scotland. We can thus de-
19 duce the expected GIC at each transformer node in the system based on the
20 network topology from an input surface electric field. We apply these devel-
21 opments to study the theoretical response of the UK high-voltage power grid
22 to modelled extreme 100- and 200-year space weather scenarios and to a scaled
23 version of the October 2003 geomagnetic storm, approximating a 1 in 200
24 year event.

1. Introduction

25 Large excess electric fields are generated in the ground during severe space weather
26 events due to the (secondary) induction effects of a changing magnetic field within a
27 conductive medium. During large geomagnetic storms, electric currents – termed Geo-
28 magnetically Induced Currents (GIC) – can flow through the ground, usually harmlessly.
29 However, high-voltage power systems can be vulnerable to GIC flow, particularly where
30 they offer a low-resistance path for the current compared to the ground. In this paper we
31 seek to simulate the flow of GIC in the UK high-voltage network using a state-of-the-art
32 ground conductivity model and the most accurate and up-to-date representation of the
33 grid characteristics and topology available.

34 The key magnetic parameter in the ‘GIC problem’ is the time rate of change of the
35 magnetic field, denoted $d\mathbf{B}/dt$, and in particular its component in the horizontal plane,
36 dH/dt [e.g. *Viljanen et al.*, 2001]. Determining the expected peak rate of change of dH/dt
37 for a region is important for GIC studies. Values of dH/dt can be readily extracted
38 from digital archives, typically recorded at a cadence of one minute. *Thomson et al.*
39 [2011] estimated likely 100- and 200-year maxima in dH/dt , using up to 30 years of
40 minute-mean digital data from 28 European observatories. They showed that peak dH/dt
41 increases with magnetic latitude, with a distinct ‘bump’ in the magnitude of dH/dt around
42 55-60°N (geomagnetic latitude), associated with an enhanced ionospheric current system
43 known as the auroral electrojet. The UK is within this region of enhanced magnetic field
44 activity and so experiences such enhancements during major geomagnetic storms.

45 Prior to 1983 in the UK, only analogue measurements recorded on paper exist, though
46 these do extend back to the 1840s and contain major magnetic storms, such as the ‘Car-
47 rington Event’ of September 1859 and the May 1921 storm [e.g. as discussed in *Kappen-*
48 *man*, 2006]. In the digital era, severe magnetic storms occurred in March 1989, November
49 1991 and October 2003. In the UK, the 1989 storm caused damage to two transformers
50 [*Smith*, 1990; *Erinmez et al.*, 2002].

51 Detailed geophysical studies of these storms, such as *McKay* [2003] and *Turnbull*
52 [2010, 2011], have modelled the impact on simplified versions of the high-voltage trans-
53 mission system of the UK. *Thomson et al.* [2005] showed that the measured GIC for the
54 2003 event was reasonably reproduced by the geophysical models of *Beamish et al.* [2002]
55 and *McKay* [2003], which were constructed for the UK mainland, also known as Great
56 Britain (GB) but most detailed in Scotland. Measured GIC in the UK during the Octo-
57 ber 2003 event reached 42A [*Thomson et al.*, 2005]. More recently, *Pulkkinen et al.* [2012]
58 have developed scenarios of realistic electric field change for a 100-year extreme event,
59 specifically to aid engineering and network planning. These were applied to the high-
60 voltage network of Virginia in the USA and also to a relatively simple model of the GB
61 high-voltage network to compute the expected GIC in the network. However, these were
62 relatively uniform electric field models, and lacked the expected spatial variation of the
63 magnetic and induced electric field. In this paper we attempt to produce a more realistic
64 representation of the induced electric field in the UK during a severe space weather event
65 and using an improved network model to compute the expected GIC for the GB power
66 grid.

67 In Section 2, we describe our new conductivity model which is based on the geophysical
68 properties of the geological structure of the UK. We then describe the methodology for
69 creating the extreme variations of the magnetic field during 100- and 200-year extreme
70 geomagnetic events using synthetic models of the auroral electrojet and a scaled version of
71 the October 2003 storm. In Section 3 we show the resulting GIC amplitudes and spatial
72 patterns generated when applied with our new model of the high-voltage transmission net-
73 work. Finally, we discuss the limitations and caveats with regards to modelling accuracy
74 and validation.

2. GIC Modelling

75 There are four main requirements for computing GIC within a electrical network: (a) a
76 model of the conductivity structure of the region (b) a detailed set of spatial and temporal
77 measurements and/or models of the magnetic field, (c) the computation of the electric
78 field from the interaction of (a) and (b), and (d) a network model of the high-voltage
79 power grid and transformers.

80 Once the surface electric field has been computed, the voltages along electrical lines
81 in a connected power grid are integrated and inverted using the network topology and
82 characteristics to calculate GIC at each transformer. These steps are described in more
83 detail in the following subsections.

2.1. UK Ground Conductivity Model

84 The penetration of the magnetic field into the ground (i.e. skin depth) is highly depen-
85 dent on the conductivity of the local region and the time period (frequency) over which
86 the change of the magnetic field occurs. The vertical distribution of the resistivity within

87 the Earth's crust, and the period considered, determine the rate of attenuation of the
88 induced electric field. Deeper layers are more significant at long periods and the shallow
89 layers produce stronger influences at short periods.

90 The interaction of the external magnetic field with the conductive Earth is approximated
91 in our code by 'thin-sheet' modelling; this determines the surface electric field arising at
92 a particular frequency from layers of conductive material in the sub-surface. The chosen
93 frequency (or period) of the rate of change of the magnetic field equates to its penetration
94 depth.

95 The thin-sheet modelling code used in this study is based upon the work of *Vasseur and*
96 *Weidelt*. [1977]. Using a series of appropriate Green's functions and integrals, the thin-
97 sheet approximation can be used to model the likely influence of near surface conductivity
98 contrasts in the context of regional induction. Hence, a thin-sheet model includes the effect
99 that lateral conductivity variations have on redistributing regional or 'normal' currents
100 induced elsewhere (e.g., oceans or shelf seas). However, a number of assumptions and
101 approximations are made to ensure that the thin-sheet model remains valid.

102 The new UK conductivity model is derived from the analysis of the conductivity prop-
103 erties of the bedrock materials, based on the British Geological Survey (BGS) 1:625,000
104 geological map of the UK and Northern Ireland. The model, described by *Beamish* [2012],
105 uses the information obtained from recent airborne geophysical surveys across the UK.
106 The results show that the effective resistivity mapped from remote sensing surveys can be
107 used to estimate conductivity across most of the UK. The methodology (see also *Beamish*
108 *and White* [2012]) provides a lithological and geostatistical assessment of the conductiv-

ities of all the UK bedrock formations. The central moments of the distributions were found to range from 8 to 3125 Ω m.

Again, there are a number of assumptions in this method, not all of which are strictly true. For example, the assumption that surface bedrock extends to depth or that rock units (sandstone, limestone, basalt etc) have uniform and constant conductivities to a depth of 3 km are clearly incorrect in many locations. However, the approximations are useful in constructing a reasonably representative regional conductivity model.

Onshore, the 1:625,000 ‘near-surface’ bedrock conductivities were used including Northern Ireland but excluding the Republic of Ireland. For the offshore regions, the bathymetry and a uniform value of sea water conductivity (4 S/m) are used. This is a very thin layer (typically < 200 m) providing the conductance which equates to the conditions of a previous existing thin-sheet model from prior work in 2002/3. Figure 1 shows the model, termed the BGS2012 Conductivity Model. At the 10 km cell size used, the model comprises 4211 values of conductance, ranging from 2 to 11598 S.

2.2. Regional Estimation of the Magnetic and Electric Fields

The temporal variation of the external magnetic field during a severe geomagnetic storm can be extremely rapid with a complex regional spatial variation. In the auroral regions, results from networks of magnetometers such as IMAGE [Viljanen and Häkkinen, 1997] or CARISMA [Mann *et al.*, 2008] show rapid temporal fluctuations and spatial rearrangement of the magnetic field associated with auroral electrojets and field-aligned currents.

In order to estimate the surface electric field, we must make assumptions about the configuration of the magnetic field during a large storm at the geomagnetic latitudes of the UK. We therefore assume that strong magnetic fields arise primarily from the

131 presence of a very strong auroral electrojet expanding southwards over the UK, driven
132 by a major geomagnetic storm. We assume the auroral electrojet generates a rapidly
133 changing external magnetic field observed on the ground. The core and crustal magnetic
134 fields are essentially static on short time scales of seconds to days and we ignore the effect
135 of the ring current as the electrojet is the largest signal at these latitudes during such
136 events. The rapidly changing external part of the magnetic field induces an electric field
137 in the Earth, and we use the horizontal, North (X) and East (Y), components to compute
138 a regional surface electric field model.

139 Two different scenarios for the spatial and temporal configuration of the magnetic field
140 were synthesised: (a) a set of idealised models of a large-scale auroral electrojet and (b)
141 a scaled version of the 2003 Halloween storm based on the interpolation of the magnetic
142 field from observatory and variometer measurements around the UK.

143 **2.2.1. Electrojet Models**

144 We developed two electrojet model profiles: the first electrojet model has an amplitude
145 profile akin to a ‘top-hat’ function, extending from 53° to 63°N in geomagnetic latitude,
146 while the second has a ‘tapered-cosine’ profile extending between 48° and 68°N in geo-
147 magnetic latitude. We use the two different models to examine if the amplitude gradient
148 (slope) of the magnetic field strongly affects the GIC. The Top Hat model gives a very
149 strong gradient across its edges while the Tapered Cosine model has a gentler gradient.
150 Two orientations of the auroral electrojet were then computed; (a) geomagnetically east-
151 west aligned across the UK and, in order to produce an orthogonal magnetic field direction,
152 (b) a second set of profiles in a geomagnetic north-south alignment (which approximately

153 follow the central axis of the UK). Note that a north-south configuration is not realistic
 154 due to the configuration of the main magnetic field.

155 The electrojet models were created as normalised values on a square grid in geomagnetic
 156 coordinates and then rotated 10° counter-clockwise to match the appropriate position over
 157 the UK in geographic coordinates. The electrojet grids were cropped and sub-sampled to
 158 $1/12$ th of a degree to match the grid-spacing of the ground conductivity model.

159 To scale the electrojet model magnetic fields to the correct amplitude for an extreme
 160 event, the results from the *Thomson et al.* [2011] study on the statistical predictions of
 161 extreme values in European magnetic observatory data were applied. Table 1 gives the
 162 predicted range in activity between $55\text{--}60^\circ\text{N}$ at 100-year and 200-year return periods.
 163 The largest measured digital (i.e. modern) dH/dt for the UK is around 1100 nT/min (in
 164 1991). Therefore we chose to use 1000 nT/min, 3000 nT/min and 5000 nT/min in this
 165 analysis to approximate the expected maximum in dH/dt for 30, 100 and 200 years.

To convert the horizontal rate of change (dH/dt) to equivalent root-mean-square (RMS)
 input horizontal field for use in the thin-sheet approximation code, we assumed the field
 amplitude was changing sinusoidally over a period of length t . Hence the RMS input field
 strength, H_0 , can be computed using the approximation:

$$dH/dt = \sqrt{2}\pi H_0/T \quad (1)$$

166 where $H = H_0 \sin(2\pi t/T)$. H_0 is the strength of the field from the electrojet and T is
 167 the period of electrojet variation (in minutes). If we assign $T = 2$ minutes, this leads
 168 to magnetic field input strengths H_0 of approximately 450 nT, 1350 nT and 2250 nT
 169 for $dH/dt = 1000$ nT/min, 3000 nT/min and 5000 nT/min. The conductivity model
 170 responds differently at different periods (or frequencies) to these magnetic field changes.

171 For this study, the response of the electric field at periods of 2 minutes (120 seconds),
172 10 minutes (600 seconds) and 30 minutes (1800 seconds) are chosen, though the spectral
173 characteristics of the external magnetic field during storms are typically broadband in
174 nature. Longer periods are regarded as insignificant for GIC hazard assessment.

175 *Thomson et al.* [2011] suggest that in Europe the extremes in H are relatively unlikely
176 to exceed 10,000 nT once every 200 years. We therefore use this as a maximum cut-off
177 for the value of H_0 . For this reason, 3000 nT/min and 5000 nT/min changes are not
178 considered to be physically reasonable as ‘worst cases’ for electrojets varying with periods
179 longer than about 10 minutes. However, we do retain them for comparison purposes.

180 We assume that the change in H is due either to the X or the Y component of the
181 external magnetic field. Table 2 shows the computed values for the horizontal component
182 of the main field corresponding to these time periods for the electrojet models.

183 There are now up to twelve different magnetic field source scenarios for electric field
184 computation per time period: (a) two electrojet profiles (Top Hat and Tapered Cosine);
185 (b) two orientations (as geomagnetically E-W and N-S aligned electrojets) and; (c) two
186 or three dH/dt scaling values (as per Table 2). The grid models were multiplied by the
187 selected H_0 values to scale them to the magnetic field strength before combining them
188 with the conductivity model to calculate the electric field strength at each point across the
189 UK mainland. Figure 2 shows an example of the magnetic field strength for the auroral
190 electrojets models scaled to 1350 nT (a 1-in-100 year scenario). For convenience, we
191 concentrate on the 120 second period for the remainder of the paper, though the models
192 for all scenarios were computed.

193 **2.2.2. Scaled October 2003 storm**

194 To generate a more ‘realistic’ representation of the spatial variation of the geomagnetic
195 field during a large storm, a model of the magnetic field during the October 2003 event
196 was constructed based upon the measurements from nine observatories and variometers
197 around the United Kingdom and North Sea region. The observatory data were downloaded
198 from the World Data Centre for Geomagnetism (Edinburgh), while the Faroes, York and
199 Crooktree variometer data were provided by the Sub-Auroral Magnetometer Network
200 (SAMNET) operated by Lancaster University.

201 The spatial variation of the magnetic field was estimated using minute-mean data in-
202 terpolated over a large region using the Spherical Elementary Current Systems method
203 [*Amm and Viljanen, 1999*], as described in detail in *McLay and Beggan [2010]*. The mag-
204 netic field values were multiplied by five to achieve a 200-year extreme event with a peak
205 maximum rate of change of approximately 5,000 nT/min. Figure 3 illustrates the varia-
206 tion at each observatory/variometer of the (scaled) horizontal components of the external
207 magnetic field for the 30th October 2003. The magnetic field was most active during the
208 period 19.00–22.00 UT. Figure 4 shows the spatial change of the strength of the horizontal
209 field components for four snapshots, including 21.20 UT, the peak of the 2003 Halloween
210 storm, as recorded in the UK.

2.3. UK High-voltage Network Model

211 National Grid UK is responsible for the operation of the high-voltage 400 kV, 275 kV and
212 132 kV transmission network across Great Britain (i.e. the mainland of the UK). The
213 transmission network consists of hundreds of step-up and step-down transformers that
214 transfer power generated typically at 22.5 kV from the source to the local distribution
215 networks for industrial, business and household consumers. The most efficient method for

216 transferring power over long distances is to step the voltage up to reduce the resistance
 217 (and hence the Ohmic heating) in the connecting transmission lines. However, if the
 218 ground resistance is sufficiently high, the low-resistance wires of the network provide an
 219 easier route for GIC to pass through the earth neutral of the connecting transformers.

In conjunction with National Grid UK, a full description of the UK high-voltage power network was developed. The data consists of latitude, longitude and electrical characteristics (earthing, transformer and line resistance) of each transformer node in the high-voltage network. These parameters are used to calculate GIC (in Amperes) along power transmission lines from the matrix equation in *Lehtinen and Pirjola* [1985]:

$$\mathbf{I} = (\mathbf{Y} + \mathbf{Z})^{-1}\mathbf{J} \quad (2)$$

220 where \mathbf{J} is the geo-voltage computed between nodes, \mathbf{Z} is the impedance matrix, \mathbf{Y} is
 221 the network admittance matrix and \mathbf{I} is the vector containing the estimated GIC at each
 222 node. The input data from the network parameters are used to calculate \mathbf{Y} and \mathbf{Z} . The
 223 geo-voltage \mathbf{J} is calculated by interpolating the electric field grid value onto the power
 224 transmission lines and integrating along the line. The GIC at each node on the grid is
 225 then computed. The GIC are calculated from both the North and East components of
 226 the surface electric field. Note that when modelling real-world data, to compute the total
 227 GIC at each node, all periods should be integrated. In this study, however, we use three
 228 discrete periods (120, 600 and 1800 seconds) only to approximate the full spectrum.

229 The 2012 model of the UK network consists of 701 transformers and 1153 connections.
 230 Some connections are very short, for example, between two transformers on the same site,
 231 while the longest is 189 km. The median line length is 10 km (mean: 17 km). Figure 5
 232 shows the UK 400 kV and 275 kV network and the 132 kV network in Scotland.

3. Results of Electric field and GIC computation

Using the ‘thin-sheet’ approximation, the excess electric field is estimated for a large area around the UK from -12° to $+2^\circ$ longitude and from 50° to 60° latitude i.e. the area is $14^\circ \times 10^\circ$ in size. This large area includes the shallow sea and deeper ocean, though excludes effects from mainland Europe. In addition to the surface layer, the model also includes an 11 layer 1-D model of the lower crust and mantle, adding a third dimension. The model has a resolution of 1/12th of a degree in latitude and longitude (approximately 10 km cell size). This gives an electric field model for each magnetic field configuration for a given period (e.g. 120 seconds).

The thin-sheet modelling code was run with the BGS2012 conductivity model using the auroral electrojet model configurations for the three different response frequencies (where applicable). Note, that an East-West aligned magnetic field (i.e. the X component) generates the North-South aligned (i.e. Y component) electric field. We concentrate on results from the shortest period events (120 seconds) as these generate the largest GIC from our modelling technique.

Figure 6 shows the output of the thin-sheet modelling for assumed 30, 100 and 200-year extreme events based on the idealised auroral electrojets. The modelled electric fields induced in the surface by a period of 120 seconds are for H_0 fields of 450, 1350 and 2250 nT from various auroral electrojet configurations are plotted. The largest field changes induce the largest surface electric fields, reaching up to 15.1 V/km in Figure 6 (lower right panel).

In Figure 7 the results of the thin-sheet modelling for four snapshot times from the 1-in-200 year storm event are shown. The modelled electric fields induced in the surface

255 by a period of 120 seconds for H_0 fields of 3918, 4454, 9420 and 1454 nT, respectively.
256 The figure shows the largest field changes induced reach up to 8.1, 10, 27.9 and 6.9 V/km
257 in Figure 7. These electric fields are similar to those modelled in *Pulkkinen et al.* [2012].

258 From the computed surface electric fields, GIC were obtained for each of the 701 trans-
259 formers in the network for each extreme scenario. Figure 8 illustrates the GIC generated
260 for a 100-year scenario for the 120 second period for the four configurations of the auroral
261 electrojet. The GIC entering the grid are shown in blue (positive), while GIC exiting into
262 the ground are in red (negative). Note, the sign of the GIC (positive or negative) is not
263 important in terms of its impact on a transformer, as it is the absolute DC bias in the
264 transformer that affects its performance.

265 Figure 9 shows the modelled GIC generated for a 200-year scenario for the 120 second
266 period from the four snapshots of the extreme storm of section 2.2.2 . The values are larger
267 than those in Figure 8 which is to be expected as the magnetic field values are larger.
268 Due to the spatial complexity of the magnetic field, the locations of large magnitude GIC
269 differ from the hypothetical electrojet model.

270 The results of the ten largest GIC at the nodes are tabulated in Tables 3 (Tapered-
271 Cosine profile) and 4 (Top-Hat profile). The tables show the output of the GIC model
272 for each expected return period, depending on the orientation of the electrojet. (For
273 commercial reasons the identity of the nodes are not given.) Note that different nodes
274 have the largest value of GIC, depending on the orientation of the electrojet and that the
275 values from the Top-Hat profile are, on average, larger.

276 The largest GIC occur in the north of the UK, and in the ‘corner’ nodes of system
277 (e.g., southwest Wales and England) or in isolated regions (Scottish Borders). Where

278 nodes lie close together, especially in the southern UK, there is a tendency for smaller
279 GIC (e.g., London/southeast England), though this is not necessarily the case in other
280 clusters of transformers (e.g., northeast England). Also, due to the different transformer
281 characteristics (e.g. from age, type, connectivity) even nodes on the same site display
282 different GIC susceptibility, indicating that the problem of understanding GIC even at a
283 single site can be subtle.

284 Although higher voltage power lines are most affected by GIC, we have found that
285 including lower voltage lines significantly modifies the electrical topology of the grid and
286 hence the paths of least-resistance for excess current. To illustrate this, we modelled the
287 GIC in the 400 kV and 275 kV lines only and compared it to the GIC computed at the
288 same transformers when the 132 kV grid in the northern UK is included. Figure 10 shows
289 the differences at the common nodes using a Tapered Cosine profile during a 100 year
290 event for a 120 second period (i.e. the electric field from Figure 6). The largest differences
291 for the East-West alignment of the electrojet (Figure 10 (a)) are located in the north of
292 the UK, vanishing in more southerly nodes. When the electrojet is north-south aligned
293 (Figure 10 (b)) the largest differences are up to about 8% of the total GIC at any given
294 site. The number of nodes affected across the region also increases slightly, with nodes
295 much further south of the 132 kV grid showing differences. This result suggests that any
296 unmodelled connectivity of the high-voltage grid to lower voltage lines will have a modest
297 effect on the size of GIC computed.

4. Discussion

298 We attempt to determine the flow of GIC in the UK power grid during the worst-case
299 scenarios of space weather that can be expected in a 200-year period. The use of idealised

300 electrojet models allows us to investigate the hypothetical response of the grid while a
301 scaled version of the 2003 Halloween storm gives a more nuanced spatial magnetic field
302 model.

303 From a comparison of the magnetic field configurations in Figures 2 and 4 it can be seen
304 that the Tapered Cosine electrojet east-west alignment (Figure 2 (upper left)) is arguably
305 a more physically realistic distribution of electrical current in the ionosphere. However,
306 the tapered cosine electrojet results in typically lower GIC than the Top Hat electrojet
307 (in Figure 8 (lower panels)).

308 Although model outputs are described in terms of both east-west ('X') and north-
309 south ('Y') scenarios, the dominant electrojet orientation is in the east-west (geomagnetic)
310 direction, particularly over prolonged periods, though over shorter intervals there can be
311 a strong north-south component. Any North-South component to the electrojet over the
312 UK (e.g. during a westward travelling surge) will on average increase the GIC flowing in
313 transformer earths. In places, this GIC can be an order of magnitude greater than that
314 for an East-West oriented electrojet. Longer period variations with significant magnitude
315 (e.g. $> 3000\text{nT}/\text{min}$) are physically less realistic, as noted in section 2.2.1, but could
316 produce large GIC if realised.

317 Analysis of the spatial distribution of the magnetic field strength during large storms
318 (e.g. October 2003) suggests that a single electrojet model is often not correct. For
319 example, Figure 4 shows a complex magnetic field distribution for 21:20 during the peak
320 of the storm. As well as a large variation in strength, the spatial variation gives rise to the
321 largest GIC occurring in the central parts of the UK (Figure 9), rather than in northern
322 regions (as occur in Figure 8).

323 One of the more interesting aspects is that the largest GIC are positive (i.e. as the
324 current enters the grid). This is due to the topology of the grid and the location of the
325 nodes, as the current tends to flow from north to south. Due to the larger number of
326 nodes in close proximity in the southern UK (where the population is densest), it appears
327 the current flowing out is divided amongst a greater number of nodes.

328 However, there are several limitations to this approach; for example, the geophysical
329 model of the auroral electrojet is idealised, as it is assumed that the periodic variations in
330 the auroral electrojet are concentrated into a discrete frequencies. This is unphysical but
331 makes the problem manageable. We also assume that the electrojet parameters (location,
332 width, strength) from the analysis of 30 years of data [*Thomson et al.*, 2011] are reasonably
333 representative during extreme events over longer time scales.

334 The thin-sheet modelling approach has various physical constraints. Short period vari-
335 ations of less than 30 seconds cannot be correctly modelled using the thin-sheet method
336 [*McKay*, 2003], as the assumptions for deriving skin-depth breaks the approximation be-
337 tween conductivity and the period of the electromagnetic wave. In reality, very rapid
338 changes of the magnetic field do not penetrate deeply into the ground.

339 The power grid itself changes over time and even the model here is simplified with
340 respect to the contemporary network. However it should provide a good indication of grid
341 response and our modelling does show that the same locations are consistently at risk from
342 particularly large GIC. This can be used to inform network engineers of potential issues
343 to monitor and allows planning and preparation to be made in the case of an extreme
344 space weather event. During an actual event, measurement of the external magnetic field

345 from local magnetic observatories can be used to provide near real-time estimates of GIC
346 from simulations based on the conductivity and network models used in this study.

5. Conclusions

347 We have investigated the generation of GIC in the high-voltage power network in the
348 UK in response to 100- and 200-year extreme geomagnetic storm scenarios. We have
349 shown how a detailed model of the UK conductivity, based on the BGS 1:625000 geological
350 database, can be used to generate surface electric field models from magnetic field changes
351 induced by idealised auroral electrojet models.

352 The GIC obtained show the theoretical response of the UK power system to an extreme
353 space weather event. This will help transmission network engineers plan for and protect
354 the grid from extreme events. Future improvements to the theoretical modelling will
355 require validation of the outputs against real GIC measurements in the network during
356 storm conditions.

357 **Acknowledgments.** This research was partly funded by NERC New Investigators
358 grant NE/J004693/1 and from the European Community's Seventh Framework Pro-
359 gramme (FP7/2007-2013) under Grant Agreement no. 260330. The Sub-Auroral Mag-
360 netometer Network data (SAMNET) is operated by the Space Plasma Environment and
361 Radio Science (SPEARS) group, Department of Physics, Lancaster University. We thank
362 National Grid for their help in constructing a detailed network model. xThis paper is
363 published with the permission of the Executive Director of the British Geological Survey
364 (NERC).

References

- 365 Amm, O., and A. Viljanen (1999), Ionospheric disturbance magnetic field continuation
366 from the ground to the ionosphere using spherical elementary current systems, *Earth
367 Planets Space*, *51*, 431–440.
- 368 Beamish, D. (2012), The 1:625k near-surface bedrock electrical conductivity map of the
369 UK, *Tech. Rep. OR/12/037*, British Geological Survey, 23pp.
- 370 Beamish, D., and J. White (2012), Mapping and predicting electrical conductivity varia-
371 tions across southern England using airborne electromagnetic data, *Quarterly Journal
372 of Engineering Geology and Hydrogeology*, *35*, 99–110, doi:10.1144/1470-9236/11-026.
- 373 Beamish, D., T. D. G. Clark, E. Clarke, and A. W. P. Thomson (2002), Geomagnetically
374 induced currents in the UK: geomagnetic variations and surface electric fields, *J. Atmos.
375 Terr. Phys.*, *64*, 1779–1792.
- 376 Erinmez, I. A., J. G. Kappenman, and W. A. Radasky (2002), Management of the geomag-
377 netically induced current risks on the national grid companys electric power transmission
378 system, *J. Atmos. Sol. Terr. Phys.*, *64*, 743–756.
- 379 Kappenman, J. G. (2006), Great geomagnetic storms and extreme impulsive geo-
380 magnetic field disturbance events: An analysis of observational evidence including
381 the great storm of May 1921, *Advances in Space Research*, *38*(2), 188–199, doi:
382 10.1016/j.asr.2005.08.055.
- 383 Lehtinen, M., and R. Pirjola (1985), Currents produced in earthed conductor networks
384 by geomagnetically-induced electric fields, *Annales Geophysicae*, *4*, 479–484.
- 385 Mann, I., D. Milling, I. Rae, L. Ozeke, A. Kale, Z. Kale, K. Murphy, A. Parent, M. Us-
386 anova, D. Pahud, E.-A. Lee, V. Amalraj, D. Wallis, V. Angelopoulos, K.-H. Glassmeier,

- 387 C. Russell, H.-U. Auster, and H. Singer (2008), The upgraded CARISMA magnetometer
388 array in the THEMIS era, *Space Science Reviews*, *141*, 413–451, doi:10.1007/s11214-
389 008-9457-6.
- 390 McKay, A. (2003), Geoelectric fields and Geomagnetically Induced Currents in the United
391 Kingdom, Ph.D. thesis, University of Edinburgh.
- 392 McLay, S., and C. Beggan (2010), Interpolation of externally-caused magnetic fields over
393 large sparse arrays using Spherical Elementary Current Systems, *Annales Geophysicae*,
394 *28*, 1795–1805, doi:10.5194/angeo-28-1795-2010.
- 395 Pulkkinen, A., E. Bernabeu, J. Eichner, B. C., and A. Thomson (2012), Generation of
396 100-year geomagnetically induced current scenarios, *Space Weather*, *10*, S04,003, doi:
397 10.1029/2011SW000750.
- 398 Smith, P. (1990), Effects of geomagnetic disturbances on the national grid system, in *Pro-*
399 *ceedings of the 25th Universities Power Engineering Conference, Aberdeen, UK*, UPEC.
- 400 Thomson, A. W. P., A. J. McKay, E. Clarke, and S. J. Reay (2005), Surface electric fields
401 and Geomagnetically Induced Currents in the Scottish Power grid during the 30 October
402 2003 geomagnetic storm, *Space Weather*, *3*, S11,002, doi:10.1029/2005SW000156.
- 403 Thomson, A. W. P., E. Dawson, and S. Reay (2011), Geomagnetic extreme statistics for
404 Europe, *Space Weather*, *9*, S10,001, doi:10.1029/2011SW000696.
- 405 Turnbull, K. (2010), Modelling GIC in the UK, *Astronomy & Geophysics*, *51*(5), 25–26,
406 doi:10.1111/j.1468-4004.2010.51525.x.
- 407 Turnbull, K. (2011), Modelling of Geomagnetically Induced Currents in the United King-
408 dom, Ph.D. thesis, University of Lancaster.

Table 1. Estimated 100 and 200 year maxima in dH/dt and H between 55° and 60° geomagnetic north summarised from Figures 5 and 6 of *Thomson et al.* [2011].

	dH/dt (nT/min)	H (nT)
100 Year Return	1000–4000	2000–5000
200 Year Return	1000–6000	3000–6500

Table 2. Static input fields to the conductivity model. (H_0 of 6825 nT and 11375 nT are regarded as relatively unlikely physical scenarios but are included for completeness.)

Return Period (Years)	dH/dt (nT/min)	1/Frequency (min)	Electrojet Field Strength H_0 (nT)
30	1000	2	450
30	1000	10	2275
30	1000	30	3820
100	3000	2	1350
100	3000	10	(6825)
200	5000	2	2250
200	5000	10	(11375)

- 409 Vasseur, G., and P. Weidelt. (1977), Bimodal electromagnetic induction in non-uniform
 410 thin sheets with an application to the northern Pyrenean induction anomaly, *Geophys.*
 411 *J. R. Astr. Soc.*, 51, 669–690.
- 412 Viljanen, A., and L. Häkkinen (1997), *Image Magnetometer Network*, p. 111, ESA Publi-
 413 cations.
- 414 Viljanen, A., H. Nevanlinna, K. Pajunpää, and A. Pulkkinen (2001), Time derivative
 415 of the horizontal geomagnetic field as an activity indicator, *Annales Geophysicae*, 19,
 416 1107–1118.

Table 3. Largest ten modelled GIC in the GB grid for a Tapered Cosine electrojet profile for a given return period and orientation. X = North; Y = East. (Units: Amperes)

Return Period (Years)	30		100		200	
	X	Y	X	Y	X	Y
1	91.9	77.0	275.6	230.9	459.3	384.8
2	72.6	68.8	217.9	206.5	363.1	344.1
3	53.1	56.5	159.2	169.5	265.4	282.6
4	40.5	43.8	121.4	131.5	202.3	219.1
5	39.6	38.3	118.8	115.0	198.0	191.7
6	37.6	31.7	112.7	-68.1	187.8	158.5
7	34.4	26.3	103.3	-74.3	172.1	131.7
8	33.2	-29.5	99.7	-88.6	-168.9	-147.7
9	-35.5	-43.8	-106.5	-131.5	-177.4	-219.1
10	-45.2	-55.5	-135.6	-166.5	-226.0	-277.5

Table 4. Largest ten modelled GIC in the GB grid for a Top Hat electrojet profile for a given return period and orientation. (Units: Amperes)

Return Period (Years)	30		100		200	
	X	Y	X	Y	X	Y
1	93.8	114.7	281.3	344.2	468.9	573.7
2	78.8	105.1	236.3	315.2	393.9	525.3
3	67.4	73.2	202.3	219.7	337.2	366.2
4	43.8	61.4	131.5	184.1	219.2	306.8
5	42.4	55.3	127.3	165.9	212.1	276.4
6	40.4	48.9	121.3	146.7	202.2	244.5
7	40.4	39.9	121.2	119.8	201.9	199.7
8	-37.1	-39.3	120.6	-117.9	200.9	-196.5
9	-42.4	-55.3	-127.3	-165.9	-212.1	-276.4
10	-55.7	-97.9	-167.2	-293.7	-278.7	-489.5

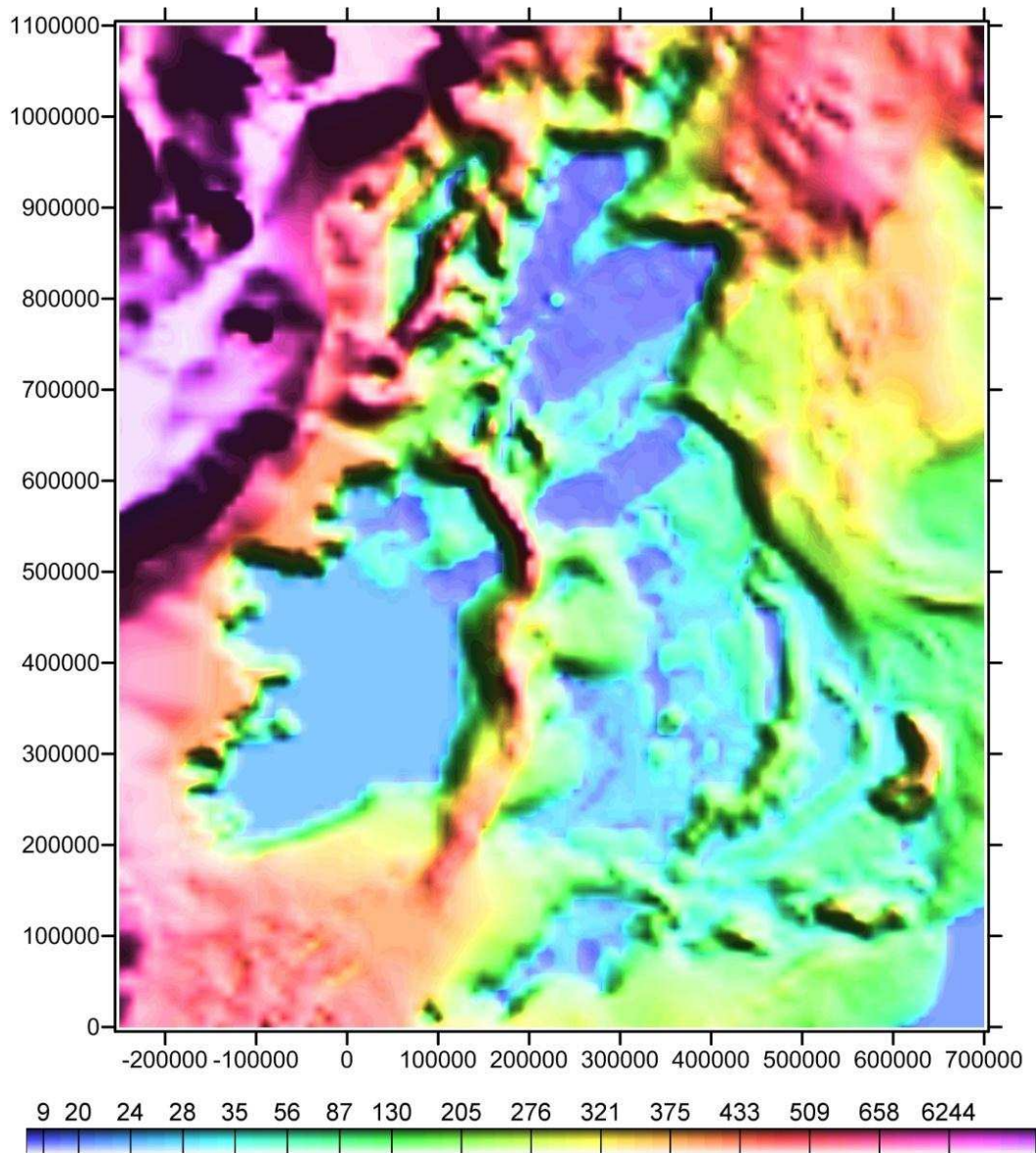


Figure 1. Conductance model (in S, 10 km resolution) of the UK based on the inferred conductivity of rock units in the British Geological Survey 1:625,000 geological database. Axis coordinates are in British National Grid (Units: m). Image uses shaded-relief (from NE) to emphasize gradients.

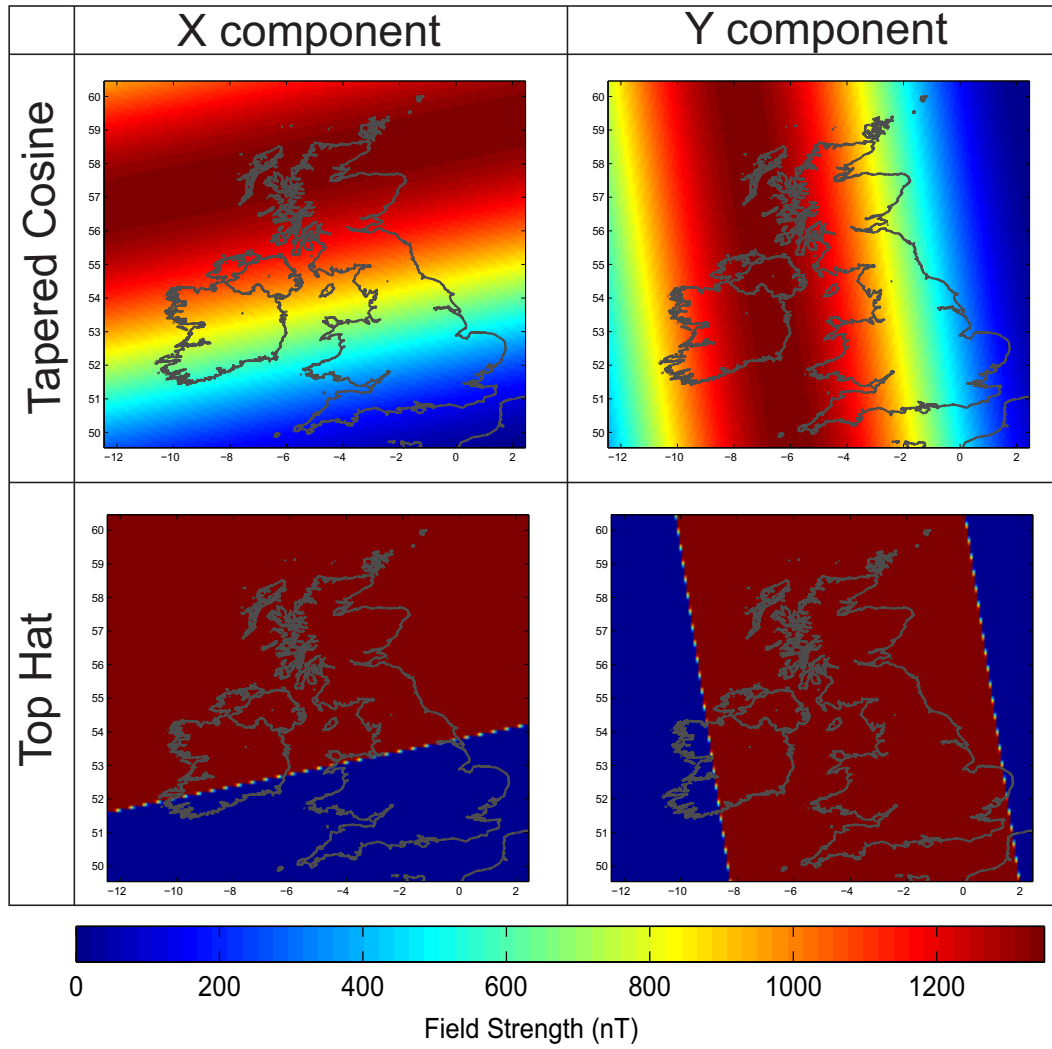


Figure 2. The horizontal components of the magnetic field from an extreme electrojet configuration.

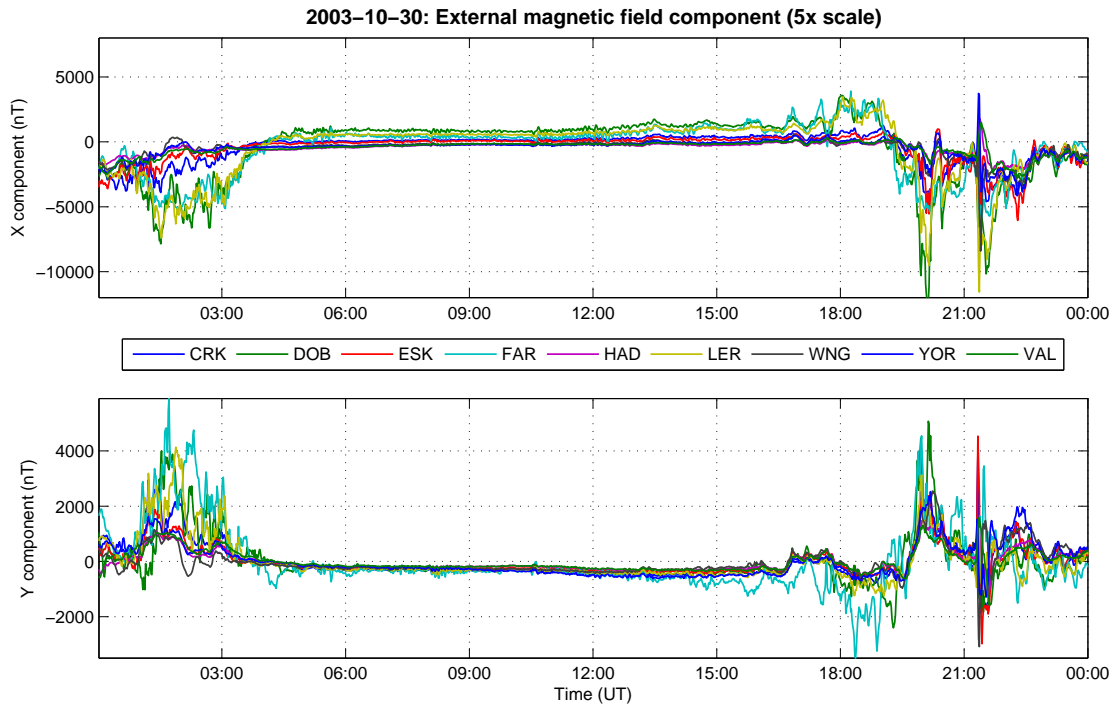


Figure 3. Time series of the $5\times$ -scaled horizontal components of the external magnetic field from the Halloween storm of 30th October 2003 geomagnetic storm. The data come from the following observatories and variometers in the region. CRK: Crooktree, DOB: Dombres, ESK: Eskdalemuir, FAR: Faroes, HAD: Hartland, LER: Lerwick, WNG: Wingst, YOR: York, VAL: Valentia.

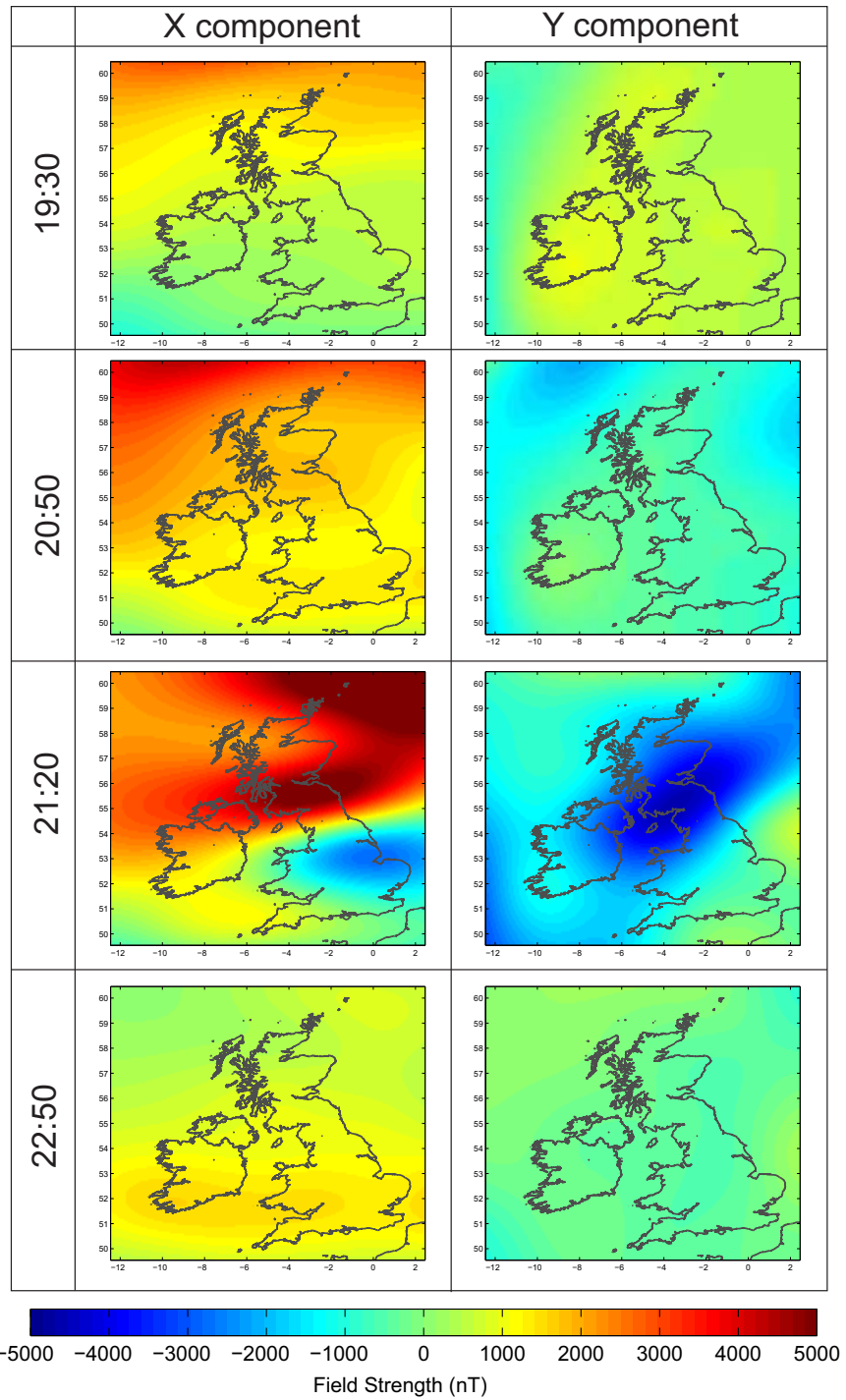


Figure 4. Snapshot of the horizontal components of the magnetic field from an extreme (approximately $\times 5$) version of the Halloween storm of 30th October 2003 geomagnetic storm. The columns show the X component (left) and the Y component (right). Nominal times in UT.

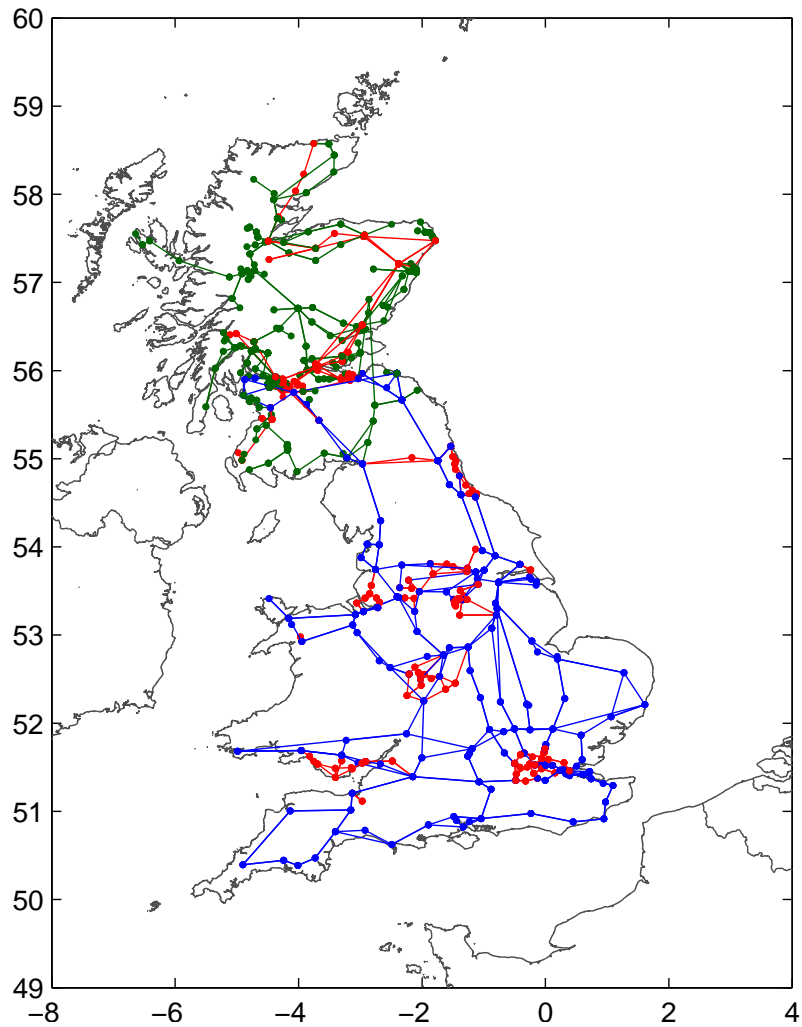


Figure 5. Network map of the National Grid GB high-voltage power grid containing 1317 transformers (dots) and 1178 connections (lines). Blue: 400 kV; red: 275 kV; green: 132 kV (Scotland only). Note, many sites host multiple transformers and connecting power lines run in parallel.

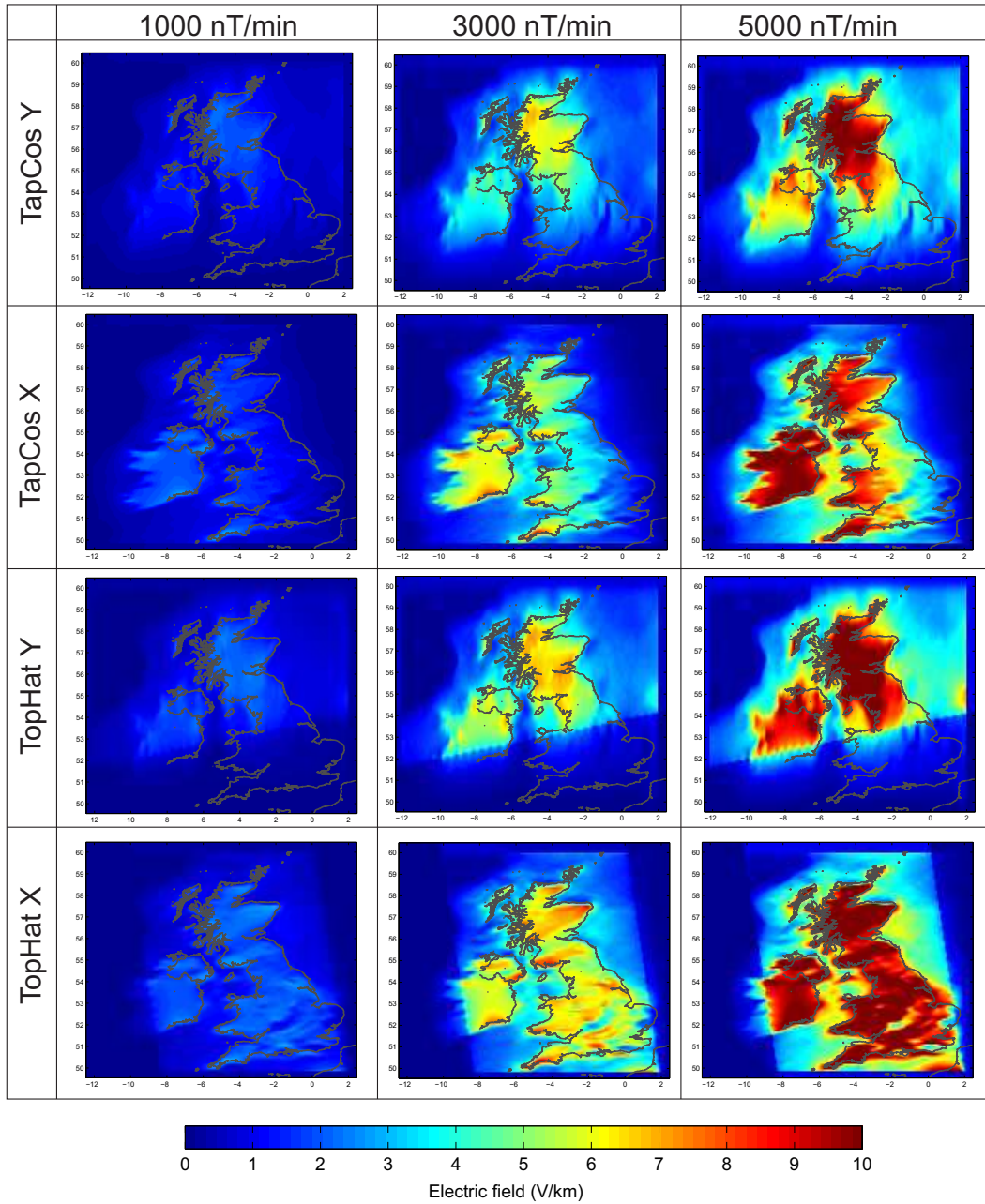


Figure 6. Electric field induced in the surface for a period of 120 seconds due to an H_0 field of 450, 1350 and 2250 nT (left to right) from an auroral electrojet model with a Tapered Cosine or Top Hat function in an East-West (X) or North-South (Y) aligned configuration.

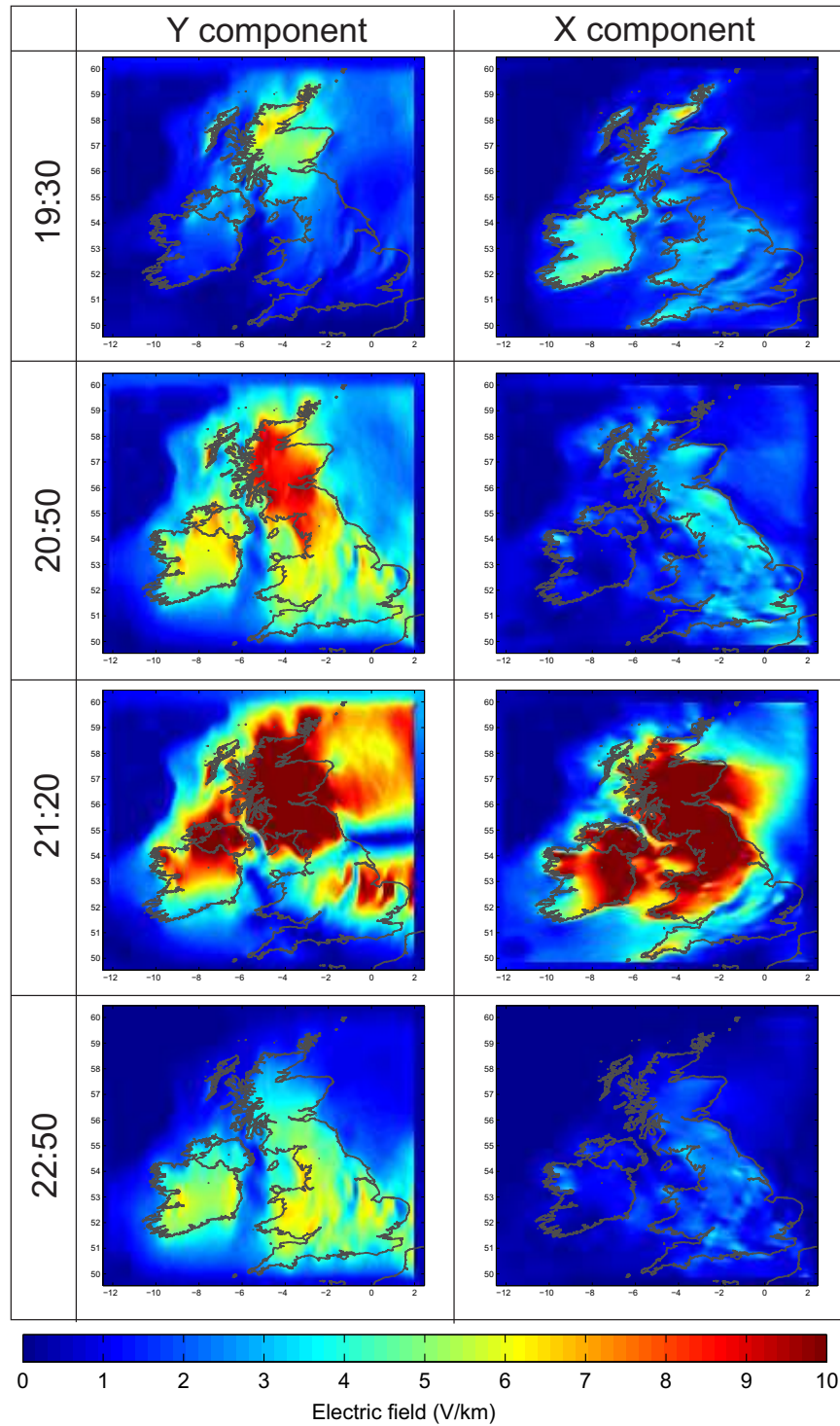


Figure 7. Electric field induced in the surface for period of 120 seconds due to magnetic fields from an extreme version of the 30th October 2003 geomagnetic storm. The columns show the Y component (left) and the X component (right). Nominal times (in UT) are illustrative, taken from the time profile of the October 2003 storm.

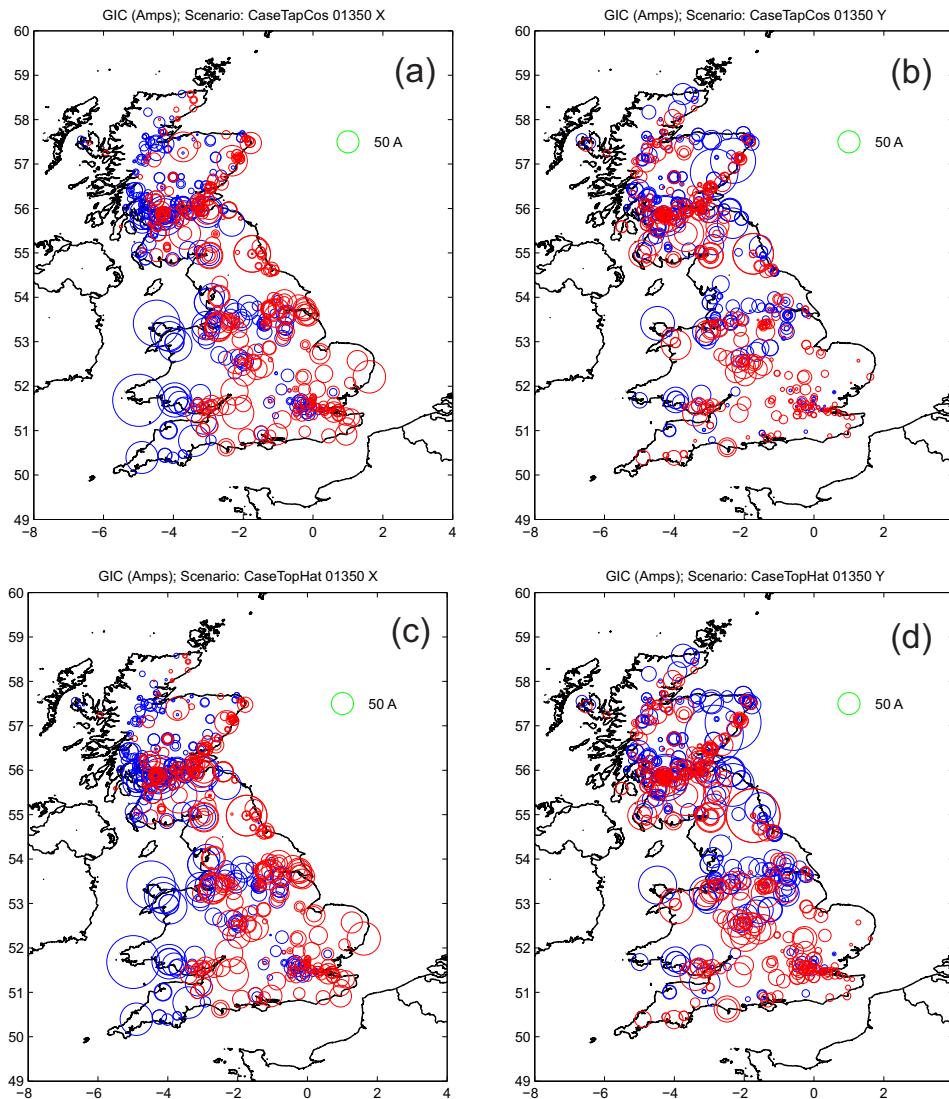


Figure 8. GIC in the National Grid GB high-voltage network due to a 100-year extreme scenario (120 second period) from an auroral electrojet with the following configurations: (a) Tapered Cosine East-West aligned; (b) Tapered Cosine North-South aligned; (c) Top Hat East-West aligned; (d) Top Hat North-South aligned. Blue indicates GIC directed into the grid, red indicates GIC into the ground. Circle size represents size (relative to scale). Note, many sites have multiple transformers present.

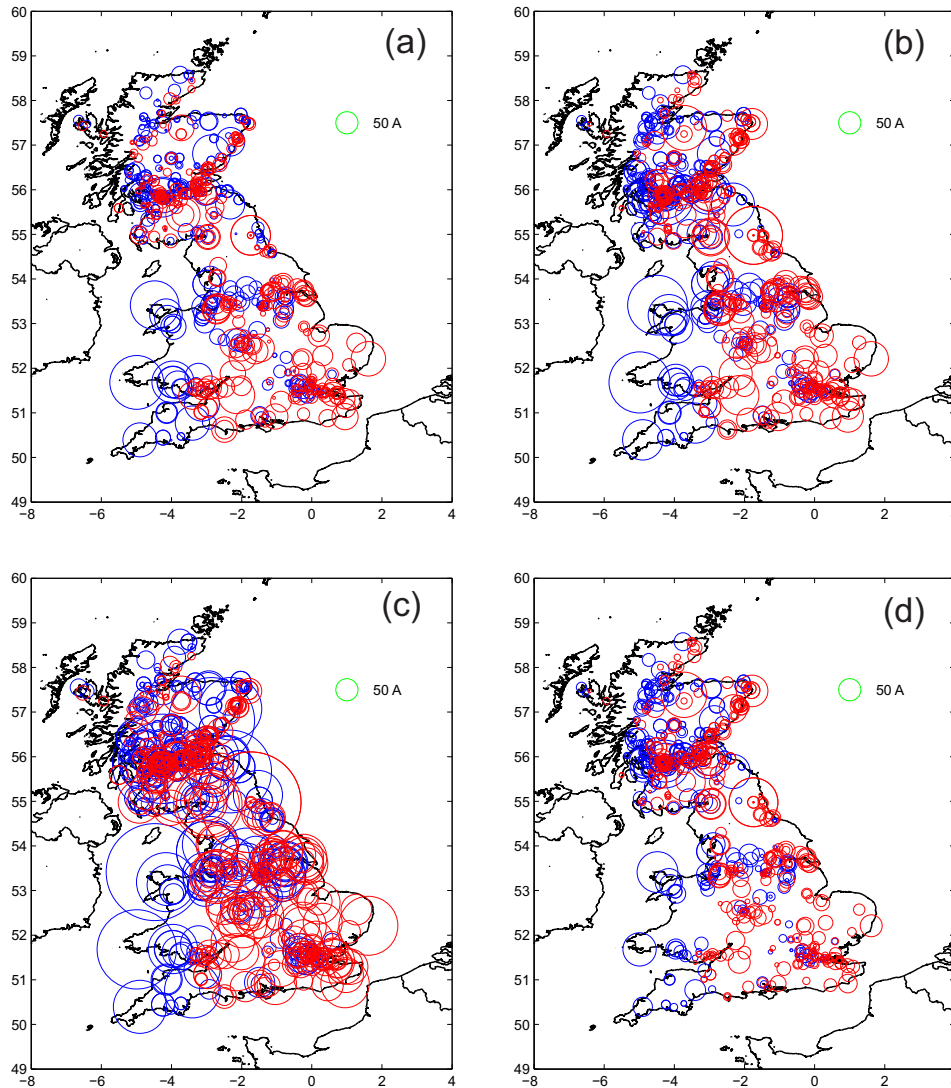


Figure 9. Snapshots of GIC in the National Grid GB high-voltage network due to an extreme storm scenario (approximately a factor of $5\times$) of the 30th October 2003 geomagnetic storm (due to an electric field with a period of 120 seconds). (a) Time: 19.30hrs; (b) Time: 20.50hrs; (c) Time: 21.20hrs; (d) Time: 22.50hrs; (see Figure 4). Blue indicated GIC directed into the grid, red indicates GIC into the ground. Circle size represents size (relative to scale).

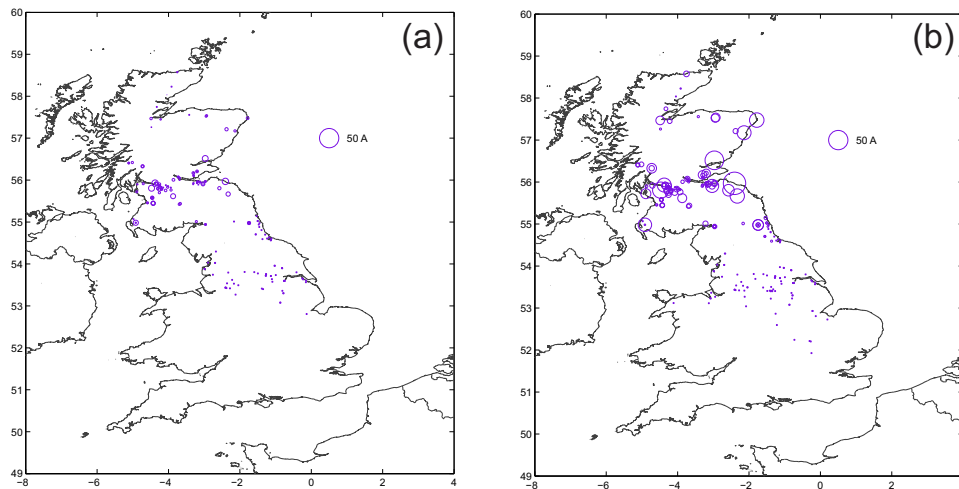


Figure 10. Differences in GIC in the 400 and 275 kV network when the 132 kV network is not included. GIC are due to a 100-year extreme scenario (120 second period) from an auroral electrojet with a Tapered Cosine profile (c.f. Figure 8 (a) and (b)): (a) East-West alignment; (b) North-South alignment; Circle size represents size (relative to scale).